RESEARCH ARTICLE

Direct Comparison of Demyelinating Disease Induced by the Daniel's Strain and BeAn Strain of Theiler's Murine Encephalomyelitis Virus

Laurie J. Zoecklein[2]; **Kevin D. Pavelko**[2]; **Jeff Gamez**[2];
Louisa Papke[2]; **Dorian B. McGavern**[4]; **Daren R. Ure**[2];
M. Kariuki Njenga[5]; **Aaron J. Johnson**[2]; **Shunya
Nakane**[1]; **Moses Rodriguez**[1,2,3]

Department of [1]Neurology and [2]Immunology, [3]Program for
Molecular Neuroscience, Mayo Medical and Graduate
Schools, Rochester, Minn.
[4] Scripps Research Institute, La Jolla, Calif.
[5] Department of Veterinary Pathobiology at University of Minnesota, Minneapolis.

We compared CNS disease following intracerebral injection of SJL mice with Daniel's (DA) and BeAn 8386 (BeAn) strains of Theiler's murine encephalomyelitis virus (TMEV). In tissue culture, DA was more virulent then BeAn. There was a higher incidence of demyelination in the spinal cords of SJL/J mice infected with DA as compared to BeAn. However, the extent of demyelination was similar between virus strains when comparing those mice that developed demyelination. Even though BeAn infection resulted in lower incidence of demyelination in the spinal cord, these mice showed significant brain disease similar to that observed with DA. There was approximately 100 times more virus specific RNA in the CNS of DA infected mice as compared to BeAn infected mice. This was reflected by more virus antigen positive cells (macrophages/microglia and oligodendrocytes) in the spinal cord white matter of DA infected mice as compared to BeAn. There was no difference in the brain infiltrating immune cells of DA or BeAn infected mice. However, BeAn infected mice showed higher titers of TMEV specific antibody. Functional deficits as measured by Rotarod were more severe in DA infected versus BeAn infected mice. These findings indicate that the diseases induced by DA or BeAn are distinct.

Introduction

Multiple sclerosis (MS) is a common disorder of the central nervous system, which is characterized by pathologic heterogeneity (35). The most often used models of MS are experimental autoimmune encephalitis (EAE) and Theiler's murine encephalomyelitis virus (TMEV). EAE and TMEV are both characterized by infiltrates of immune cells into the CNS as well as immune mediated demyelination. However, the target of the immune system is unique in both models, and consequently the pathologies of the 2 models are also distinct (8). The EAE model has been favored as an autoimmune model of MS and is often used by those supporting the autoimmune hypothesis of MS. The TMEV model has been used primarily as support for the hypothesis that immune injury to CNS cells is secondary to a persistent infectious antigen. More recently, TMEV has been shown to have an autoimmune component late in the course of disease mediated by myelin specific CD4+ T-cells (54), in contrast there is also evidence that neurologic deficits and axonal injury in the spinal cord are caused by a CD8+ T-cell driven response to virus antigen. Therefore as in MS both CD4+ and CD8+ T-cells contribute to demyelination and neurologic deficits.

Theiler's murine encephalomyelitis viruses are a group of picornaviruses that persist in the central nervous system of susceptible mice and cause a white matter inflammatory disease similar to MS (7, 46). Theiler's viruses can be subdivided into the neurovirulent subgroup GDVII, that causes lethal encephalitis after intracranial infection or the less virulent subgroup TO, which causes sub-lethal encephalitis, which is consequently cleared and develops into a persistent infection in the spinal cord white matter (24). The Daniel's (DA) (16) and BeAn (22) strains of TMEV are both members of the TO subgroup. Both strains of virus have been used as models of inflammatory demyelination in the spinal cord and as models of multiple sclerosis (26, 31). Molecular characterization of these viruses has determined that these strains share identity in 92% of nucleotides and 94% of amino acids (36). This homology is further demonstrated in the CNS disease produced by each of these viruses. These similarities include clearance of the early neuronal disease in the brain (33, 52), development of inflammatory demyelination in the spinal cord (20), persistence of virus antigen and RNA in the white matter (47, 51, 55) progressive neurologic deficits beginning months after infection (27, 31), and susceptibility or resistance to chronic demyelinating disease in various

Corresponding author:
Moses Rodriguez, MD, Mayo Clinic, 200 First St. S.W., Department of Immunology, Guggenheim (4), Rochester, MN 55905 (e-mail: rodriguez@mayo.edu)

strains of mice (3, 22, 29). In both DA and BeAn infections, the Class I MHC H-2D region plays the major role in genetically determining susceptibility or resistance (7, 46). However, there have been a number of differences noted. These include development of strong DTH responses to virus in mice infected with BeAn (5), persistence of virus antigen primarily in macrophages following BeAn infection (23) in contrast to oligodendrocytes and macrophages following DA infection (47, 50), evidence that BeAn infection mediates an autoimmune response directed against myelin antigens (54) in contrast to DA infection where direct glial cell injury and a cytotoxic responses against infected cells have been proposed to contribute to demyelination and neurologic deficits (14, 19).

Another complexity has been the strains of mice used by various laboratories. Previous results in the BALB/c strain have shown that the disease induced by TMEV in different substrains can be quite different (32). We considered this an important finding that needed to be investigated further in the two SJL substrains infected with either DA or BeAn substrains of TMEV. Early work using TMEV focused on infection of SJL/J mice from the Jackson Laboratories (21). However, more recently investigators have used SJL mice from Harlan Laboratories (SJL/JCrHsd) as the host for BeAn infection (37).

Most of the focus in understanding the pathogenesis of TMEV-induced demyelination has been focused on the pathologic studies in the spinal cord. In contrast, to the many studies investigating the pathology in the spinal cord after infection, pathologic disease in the brain has been ignored by most investigations (10, 39, 48). It has been assumed that the neurologic deficits observed in chronically infected mice are secondary to demyelination and/or axonal injury in the spinal cord (5, 26), however, there is strong evidence that pathology also occurs in the brain stem following Theiler's virus infection, which could be a major cause of functional deficits (10). Our goal was to contrast the contribution of brain pathology following infection with either DA or BeAn.

Because of the differences observed in the literature between BeAn and DA demyelinating diseases we carried out a comprehensive analysis of the CNS pathology induced by these 2 models. Our goal was to replicate the models as described in the literature rather than to evaluate the potency of these viruses. We also felt that the differences may go beyond the viruses themselves, therefore we also performed a detailed comparison of the pathologic disease in the CNS of SJL mice obtained from Jackson Laboratories or from Harlan Laboratories.

Materials and Methods

Virus. The Daniel's strain of TMEV (DA) was originally obtained from Dr Raymond Roos, University of Chicago, Ill. The virus was propagated in BHK-21 cells as described previously (47). Briefly, supernatants from BHK infected cells were sonicated, clarified by centrifugation and stored at -70°C until the time of assay. The BeAn 8386 virus used for injection into mice was obtained from Dr Stephen Miller at Northwestern University. Plaque assays were performed on L2 cells for both viruses to confirm titer. All dilutions were done in triplicate. The titer of the DA virus used for infection was 2×10^8 plaque-forming units/ml (pfu/ml) and the titer of BeAn 8386 was 5×10^7 pfu/ml. Viruses were injected at a dosage that was within the range of previously published results (33, 54). We used intracerebral inoculation of 1.5×10^6 pfu of BeAn 8386 in 30 μl of DMEM and 2×10^6 pfu of DA in 10 μl of DMEM.

Purified DA used for delayed-type hypersensitivity (DTH) was prepared from BHK-21 infected cells by ultracentrifugation on sucrose and cesium chloride gradients as described previously (47). Purified BeAn was prepared from BHK-21 infected cells and purified by sucrose gradient ultracentrifugation. Both viruses were inactivated by exposure to ultraviolet (UV) light for 10 minutes.

Mice. Female SJL/J mice and C57BL6J mice were obtained from the Jackson Laboratory (Bar Harbor, Me). Female SJL/JCrHsd mice were obtained from Harlan Laboratories (Indianapolis, Ind). Mice were 6 to 10 weeks of age at time of intracerebral infection. Mice were provided food and water *ad libitum* and all procedures conformed to National Institutes of Health and Mayo Institutional guidelines for animal welfare.

Harvesting, and morphology of the CNS. At various time points after infection (21, 45, 90, 180 days), mice were perfused with Trump's fixative via intracardiac puncture (6, 11, 38). Spinal cords were dissected and cut into one mm blocks. Every third block was embedded in glycol methacrylate and stained with a modified erichrome stain with a cresyl violet counterstain (43) to detect inflammation and demyelination. The rest of the spinal cord blocks were embedded in paraffin for immunoperoxidase staining specific for virus antigen. Detailed morphologic analysis was performed on 10 to

15 coronal spinal cord sections from each animal. A total of 2366 spinal cord quadrants from a total of 182 mice were studied. All slides were coded. Each quadrant from every third spinal cord block from each animal was scored for the presence or absence of gray matter disease, white matter inflammation and demyelination without knowledge of mouse strain or virus strain. The score was expressed as a percent of the total number of quadrants with a particular abnormality. A maximum pathologic score of 100 indicated that there was disease in every quadrant of every spinal cord block from a particular mouse (40).

Brain pathology. Brain pathology was assessed at days 21, 45, 90, and 180 p.i. Following perfusion with Trump's fixative, 2 coronal cuts were made in the intact brain at the time of removal from the skull (one section through the optic chiasm and a second section through the infundibulum) (10). The resulting slides were then stained with hematoxylin and eosin. Pathologic scores were assigned without knowledge of experimental group to the following areas of the brain: cortex, corpus callosum, hippocampus, brainstem, striatum, and cerebellum. Each area of the brain was graded on a scale of 0 to 4 as follows: 0=no pathology; 1=no tissue destruction but only minimal inflammation; 2=early tissue destruction (loss of architecture) and moderate inflammation; 3=definite tissue destruction (demyelination, parenchymal damage, cell death, neurophagia, neuronal vacuolation); 4=necrosis (complete loss of all tissue elements with associated cellular debris). Meningeal inflammation was assessed and graded as follows: 0=no inflammation; 1=one cell layer of inflammation; 2=two cell layers of inflammation; 3=three cell layers of inflammation; 4=four or more cell layers of inflammation. The area with maximal extent of tissue damage was used for assessment of each brain region.

Assessment of functional disease using an accelerated rotarod assay. The Rotamex rotarod (Columbus Instruments, Columbus, Ohio) measures balance, coordination, and motor control and was used to assess neurologic function in this study. The rotarod consists of a suspended rod powered by a variable speed motor capable of running at a fixed speed or accelerating a constant rate. Mice were trained and tested according to the protocol established previously (27). Prior to injection with TMEV each mouse received 3 days of training using a constant speed protocol. This consisted of three 3-minute trials over 3 days (12 rpm on day 1, 13 rpm on

day 2, and 14 rpm on day 3). Mice were then tested using an accelerated assay (initial speed of 10 rpm accelerating at 10 rpm per minute until the mouse fell off). The maximum speed was 70 rpm at 6 minutes. Rotarod performance was measured at 24 to 29, 46, 99, and 191 days following virus infection. All subsequent trials consisted of one day of accelerated speed testing (3 trials consisting of initial speed of 10 rpm and accelerating at 10 rpm per minute until the mouse fell off). The speed (rpm) at the time of fall was recorded for each mouse, and data were expressed as the percent decrease from baseline. For baseline we used the speed of fall at the 24-29 day time point. This allowed for the evaluation of motor performance as a result of demyelination and thus excluded any contributing deficits due to the early encephalitis. Ratios of 46, 99, and 191 day infected to 24 to 29 day infected measurements were calculated by dividing the means of the 46, 99, and 191 day performances by the mean of the 24 to 29 day performance.

Delayed type hypersensitivity (DTH) responses to virus. Mice were challenged with an intradermal injection in the pinna of the ear with purified, UV-inactivated DA in a 10 uL volume or with purified, UV-inactivated, BeAn in a 10 uL volume. Pre-challenge ear thickness measurements were taken with a Peacock dial gauge G-50 micrometer (Ozaki Manufacturing Co.) and expressed in mm^{-2}. Post-challenge measurements were taken at 24 and 48 hours post-injection.

TMEV Specific IgG enzyme linked immunosorbent assay (ELISA). Whole blood was collected from mice at time of sacrifice, and sera were isolated and stored at -80°C. Total serum IgGs against TMEV were assessed by ELISA as described (34). DA or BeAn virus was adsorbed to 96-well plates (Immulon II; Dynatech Laboratories Inc., Chantilly, Va) and then blocked with 1% bovine serum albumin (BSA; Sigma Chemical Co., St. Louis, Miss) in PBS. Serial serum dilutions were made in 0.2% BSA/PBS and were added in triplicate. Biotinylated anti-mouse IgG secondary antibody was used for detection (Jackson Immunoresearch Laboratories, Westbury, NY). Signals were amplified with streptavidin–alkaline phosphatase (Jackson Immunoresearch Laboratories) and detected using *p*-nitrophenyl phosphate substrate. Absorbances were read at 405 nm and plotted against serum dilution factors.

RNA isolation. The brain and spinal cords were removed from animals at 45 days after TMEV infection in SJL/J and SJL/JCrHsd mice. Total RNA was extract-

ed from brain and spinal cord. Briefly, the tissues were frozen and stored in liquid nitrogen. Tissues samples were homogenized in the RNA STAT-60 (1 ml / 100 mg tissue) (TEL-TEST, Inc., Friendswood, Tex) with a homogenizer, and total RNA was isolated according to the manufacturer's recommendations. The RNA concentrations were determined by spectrophotometer. The RNA samples were equilibrated to a concentration of 0.25 μg/μl and stored at -80ºC.

RT-PCR and real-time analysis. The VP2 fragment of Theiler's murine encephalomyelitis viruses (TMEV), a viral capsid region of DA or BeAn virus was amplified by RT-PCR using gene-specific primers. The primer pair sequences for VP2 of DA virus were as follows: forward (5′-TGGTC GACTC TGTGG TTACG-3′) and reverse (5′-GCCGG TCTTG CAAAG ATAGT-3′). The primer pair sequences for VP2 of BeAn were as follows: forward (5′-TGGTC GACTC TGTGG TTACG-3′) and reverse (5′-TGCCA TTGGT TCTGG TGGTT C-3′). Gluceraldehyde-3-phosphate dehydrogenase (GAPDH) was used as a control for inter sample variability. The sequences used for assaying the presence of GAPDH were: forward (5′-ACCAC CATGG AGAAG GC-3′) and reverse (5′-GGCAT GGACT GTGGT CATGA-3′). Sizes of PCR products amplified with primers for analysis were: VP2 of DA virus, 238 base pairs (bp); VP2 of BeAn virus, 573 bp; GAPDH, 236 bp.

Gene copy standards were generated with each set of samples. Standards were generated by serial 10-fold dilutions of plasmid cDNA. Standards were amplified in parallel with unknown samples by real-time quantitative RT-PCR using the LightCycler (Roche, Indianapolis, Ind). Analysis to generate standard curves was performed using LightCycler 3 software. Negative controls (omitting input cDNA) were also used in each PCR run to confirm the specificity of the PCR products. PCR products curves were linear across serial 10-fold dilutions, and the melting curve analysis indicated synthesis of a single homogenous product of the expected melting temperature. The reactions were done in 20 μl capillaries 7.0 mM Mg^{2+}, 10 pM concentrations of each forward and reverse primer, 4.0 μl of LightCycler-RT-PCR Reaction Mix SYBR Green I (LightCycler-RNA Amplification Kit SYBR Green I; Roche), 2 μl of resolution solution, 0.4 μl of LightCycler-RT-PCR Enzyme Mix, sterile H_2O, and 0.5 μg total RNA. Reaction conditions for RT-PCR for VP2 and GAPDH were as follows: reverse transcription at 55°C for 10 minutes, followed by denaturation at 95°C for 2 minutes, followed by 40 cycles of amplification. Amplification conditions were;

denaturing at 95°C at 20°C per second without plateau phase, annealing at 57°C for 7 seconds, and extension 72°C for 15 seconds. The accumulation of products was monitored by SYBR Green fluorescence at the completion of each cycle. There was a direct relationship between the cycle number at which accumulation of PCR products became exponential and the log concentration of RNA molecules initially present in the RT-PCR reaction. The reaction conditions for melting curve analysis were as follows: denaturation to 95°C at 20°C per second without plateau phase, annealing at 60°C for 5 seconds, and denaturation to 95°C at 0.1°C per second, with continuous monitoring of SYBR Green fluorescence. RNA samples (n = 76) from DA virus infected SJL/J and SJL/JCrHsd mice, and BeAn virus infected SJL/J and SJL/JCrHsd mice were analyzed for GAPDH mRNA levels to determine the levels of mRNA per sample and the technical reproducibility. The GAPDH mRNA level per sample was $\log_{10}$ 7.11 ± 0.019 (mean ± the SEM), with range from 7.58 to 6.81. Therefore, the marked variations in viral RNA levels in individual specimens could not be attributed to differences in amplifiable material. The amount of viral RNA was expressed as $\log_{10}$ virus copy number per 0.5 μg RNA total.

Immunochemistry for viral antigen. For immunohistochemical staining of TMEV antigen, brain and spinal cord sections were embedded and cut in paraffin. Slides were deparaffinized in xylol, then rehydrated through a series of ethanol rinses (absolute, 95%, 70% and 50%) prior to the addition of primary antibody. Slides with brain or spinal cord slices (5-μm thick) were incubated with a polyclonal rabbit-antiserum to purified Daniel's strain TMEV that specifically reacts with all structural proteins of TMEV (47). Slides were then incubated with a biotinylated secondary antibody and detection was performed using the avidin biotin immunoperoxidase system (Vector Laboratories, Burlingame, Calif). Quantitative analysis was performed using a Zeiss microscope attached to a camera lucida on a ZIDAS (Carl Zeiss Inc., Oberkochen, Germany) digitizing tablet. Spinal cord areas were traced to determine total gray matter area (mm^2) and total white matter area (mm^2). The number of virus antigen-positive cells for each mouse was counted and expressed per mm^2 of white matter area.

Co-localization of TMEV and CNS antigens by double-immunofluoresence staining. Brains and spinal cords were removed from 45 and 90 day TMEV

infected SJL/J mice and were snap frozen in OCT compound on brass chucks. Brain and spinal cord sections were cut at 6 microns and placed on Superfrost Plus slides (Fisher Scientific, Pittsburgh, Pa). Sections were fixed in cold filtered 95% ethanol for 5 minutes and then rinsed in phosphate buffered saline (PBS). Slides were then incubated with a polyclonal rabbit-antiserum to purified DA (47) for one hour at ambient temperature. They were then rinsed in PBS and incubated with primary antibodies to macrophage, oligodendrocyte and astrocyte markers. Rat anti-mouse F40/80 (Serotec, Oxford, United Kingdom) was used to identify macrophages, a mouse monoclonal to CNPase (Sigma, St. Louis, Miss) was used to identify oligodendrocytes and a directly labeled mouse anti-GFAP-Cy3 antibody (Sigma, St. Louis, Miss) was used to identify astrocytes. Colocalization of macrophages to virus was obtained by incubating sections with a biotinylated anti-rabbit secondary (Vector Laboratories, Burlingame, Calif) and an incubation with streptavidin-alexa fluor 594 conjugate (Molecular Probes, Eugene, Ore) for virus and macrophages were identified by incubation with an anti-Rat FITC conjugated secondary (Vector Laboratories, Burlingame, Calif). Oligodendrocytes were identified by incubating sections with a goat anti-mouse IgG-FITC conjugated secondary and virus within those cells was identified by labeling with goat anti-rabbit IgG Texas Red labeled secondary (Jackson ImmunoResearch, West Grove, Pa). Colocalization to astrocytes was obtained by incubating with an anti-rabbit-FITC conjugated secondary. Slides were post-fixed in 4% paraformaldehyde and mounted in Vectashield mounting medium (Vector Laboratories, Burlingame, Calif).

Flow cytometric analysis. A percol gradient was used for isolating lymphocytes from the CNS for use in flow cytometric analysis (18). 10^6 cells were isolated from 3 pooled C57BL/6 mouse brains infected with either DA or BeAn strain of TMEV. Cells were stained with R-phycoerythrin $D^b/VP2_{121-130}$ tetramer for one hour, adding anti CD8 PerCp, anti-CD4 APC during the final 20 minutes. In parallel experiments with the same samples, cells were stained for 20 minutes with anti-CD11b (Mac1) FITC, anti-B220 R-phycoerythrin, anti-Pan NK R-phycoerythrin and anti-CD4 APC. Anti-CD4 APC was included in all samples as a standard that all other cell types were normalized to. We thus determined the relative frequencies of various immune cells to one another. This assay, excluding $D^b/VP2_{121-130}$ tetramer staining, was also performed on 7-day infected SJL/J mice. All antibodies were purchased from BD Pharmin-
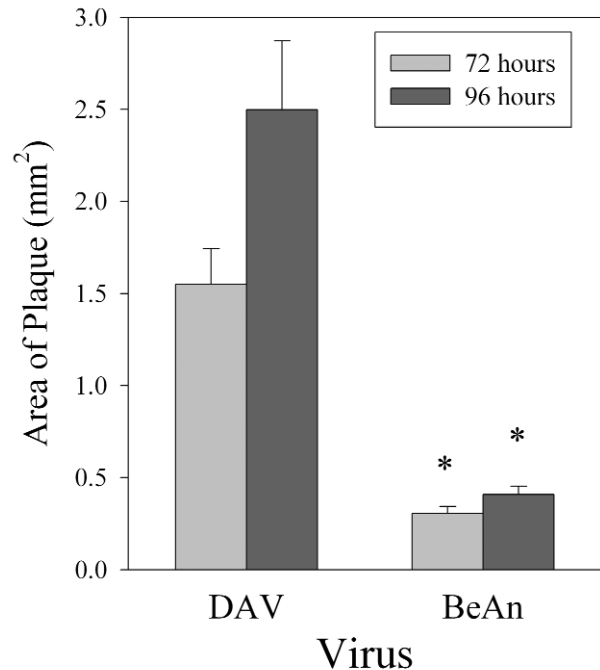

Figure 1. Area of plaques following infection of L2 cells with BeAn or DA for 72 and 96 hours. Asterisk denotes significant difference in plaque size when comparing plaques from DA and BeAn infected cells (P<0.05 by Mann-Whitney Rank Sum test).

gen (San Diego, Calif). Samples were then washed twice with FACS buffer (1% bovine serum albumin and 2% sodium azide), resuspended in cold PBS and fixed in 1% paraformaldehyde. Samples were analyzed on a Becton Dickinson FACScan instrument (Mountain View, Calif). All staining with D^b/VP2 tetramer was corrected by subtracting the background staining of the irrelevant D^b/E7 tetramer staining. D^b/E7 tetramer usually stained less than 3% of CNS infiltrating CD8$^+$ T-cells, yet bound greater than 99% of D^b/E7 epitope specific CD8$^+$ T-cells (28). To calculate relative frequencies of lymphocyte subsets, the total number of a particular lymphocyte subset was divided by the sum of the total numbers observed in all lymphocyte subsets.

Statistics. Multi-group comparisons for normally distributed data were analyzed using one way ANOVA, with pairwise comparisons done by either the Student-Newman-Keuls method for inter-group comparison or by Tukey's method for comparison to control group. Multi-group comparisons with two variables were analyzed by two way ANOVA. A repeated measures ANOVA was used to compare serial or temporal data. Comparisons between 2 individual groups were ana-

Mouse Strain	Virus Strain	Day	N	Mice + for Demyelination	White Matter Inflammation	Demyelination
SJL/J	DA	21	10	7/10	6.8 ± 2.2]b	4.7 ± 2.0]b
SJL/J	BeAn	21	10	2/10	1.6 ± 0.6	1.2 ± 0.9
SJL/JCrHsd	DA	21	14	14/14]a	10.8 ± 2.0]b	14.9 ± 2.1]b
SJL/JCrHsd	BeAn	21	9	1/9	4.1 ± 2.3	0.9 ± 0.9
SJL/J	DA	45	17	17/17]a	23.6 ± 3.7]c	24.9 ± 4.1]c
SJL/J	BeAn	45	31	21/31	15.5 ± 3.2	18.1 ± 4.1
SJL/JCrHsd	DA	45	7	7/7	23.9 ± 5.3	31.8 ± 5.2
SJL/JCrHsd	BeAn	45	10	6/10	16.6 ± 5.3	19.7 ± 7.2
SJL/J	DA	90	10	10/10]a	34.7 ± 7.2]c	48.1 ± 8.0]c
SJL/J	BeAn	90	11	5/11	8.3 ± 5.0	12.6 ± 7.2
SJL/JCrHsd	DA	180	5	5/5	28.0 ± 4.4	71.7 ± 7.5
SJL/JCrHsd	BeAn	180	7	4/7	13.2 ± 6.5	32.2 ± 15.2
C57 BL/6J	DA	45	9	0/9	0.0 ± 0.0	0.0 ± 0.0
C57 BL/6J	BeAn	45	8	1/8	0.4 ± 0.4	0.4 ± 0.4
C57 BL/6J	DA	90	12	0/12	0.0 ± 0.0	0.0 ± 0.0
C57 BL/6J	BeAn	90	12	0/12	0.0 ± 0.0	0.0 ± 0.0

Table 1. Spinal cord pathology in SJL/J, SJL/JCrHsd or C57/BL6 mice infected with either DA or BeAn strains of TMEV. N = number of mice; [a] = Significant by Fisher Exact Test ($p < 0.05$); [b] = Significant by Student's T-test ($p < 0.05$); [c] = Significant by Mann-Whitney Rank Sum Test ($p < 0.05$).

lyzed using either the Student's t-test for normally distributed data, or the Mann-Whitney Rank Sum test for data that were not normally distributed. Comparisons of incidence of demyelination were analyzed by the Fisher Exact test. Statistical significance is reported at P<0.05.

Results

DA infection generates larger plaques than BeAn in L2 cells. A comparison of the amino acid sequences of each viral protein from BeAn and DA shows that there is approximately 88 to 100% identity and 94 to 100% homology in the various regions (L, VP 4, VP 2, VP 3, VP 1, 2A, 2B, 2C, 3A, 3B, 3C, 3D) of the viruses (36). Homology was determined by hydrophobic and structural similarities between amino acids. Differences were scattered among the various regions of the viral genome. To assure that we were comparing the models accurately and that the viruses were replicating in a similar manner, we plaqued DA and BeAn to confirm the titer. BeAn was titered at 5×10^7 pfu/mL and this aliquot was used for all subsequent BeAn experiments. DA virus was titered at 5×10^8 pfu/mL. DA consistently made larger plaques than BeAn virus when placed on L2 cells. Plaques were 5-fold larger in area in DA infected cells as compared to BeAn (Figure 1) infected cells at both the 72 and 96 hour time point after infection (P<0.05 by Mann-Whitney Rank Sum test).

C57/BL6 mice are resistant to both DA and BeAn induced demyelination in the spinal cord. One very consistent feature of TMEV infection is the resistance to spinal cord demyelination in mice of H-2[b] haplotype. Immunogenetic experiments have demonstrated that resistance maps to the class I-H-2D[b] locus. In addition transgenic expression of D[b] or D[d] molecules confers resistance to mice of susceptible haplotype (2, 45). Previous work by our laboratory has demonstrated immunodominance of a VP2$_{121-130}$ peptide response in infiltrating in CD8+ T-cells in the CNS of C57BL/6J mice following DA infection (4, 9, 13). The present experiments showed similar immunodominant response present in the CNS of C57BL/6J mice after BeAn or DA infection. Seven days following infection of H-2[b] mice, CNS infiltrating cells were isolated by percol gradient and stained by FACS using a CD8 antibody and D[b]-VP2
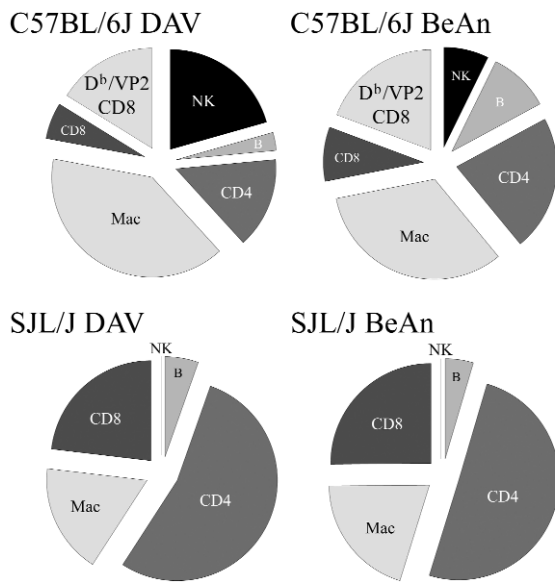
Figure 2. FACS analysis of brain infiltrating mononuclear cells (CD4, CD8, NK, macrophages and B cells) isolated at 7 days following infection of C57BL/6J mice and SJL/J mice infected with DA or BeAn virus. Cells in C57BL/6J mice were also double stained with an antibody to CD8 and VP2-tetramer.

tetramer (Figure 2). No significant difference in the number of VP2 + CD8+ T-cells was observed when comparing DA infection with BeAn infection.

We then analyzed the number of CD4, CD8, NK, macrophages and B cells infiltrating the brain 7 days after infection of C57BL/6J mice with DA versus BeAn. No differences were seen when comparing the 2 virus strains. We also analyzed the inflammatory cells infiltrating the CNS of SJL/J mice infected for 7 days with DA versus BeAn (Figure 2). No differences were observed when comparing the virus strains. However, C57BL/6J consistently had a greater percentage of CD8+ T-cells in the CNS than SJL/J after infection with either of the viruses. In contrast, a higher percentage of brain infiltrating cells were CD4+ T-cells in the CNS of SJL/J mice. We also analyzed the spinal cord of C57BL/6J mice infected with DA and BeAn at 45 days and 90 days after infection. No demyelination was observed following infection with either virus strain (Table 1).

Delayed type hypersensitivity (DTH) responses against viruses following DA and BeAn infection. There is strong evidence that TMEV infected SJL/J mice mount a strong DTH response directed against
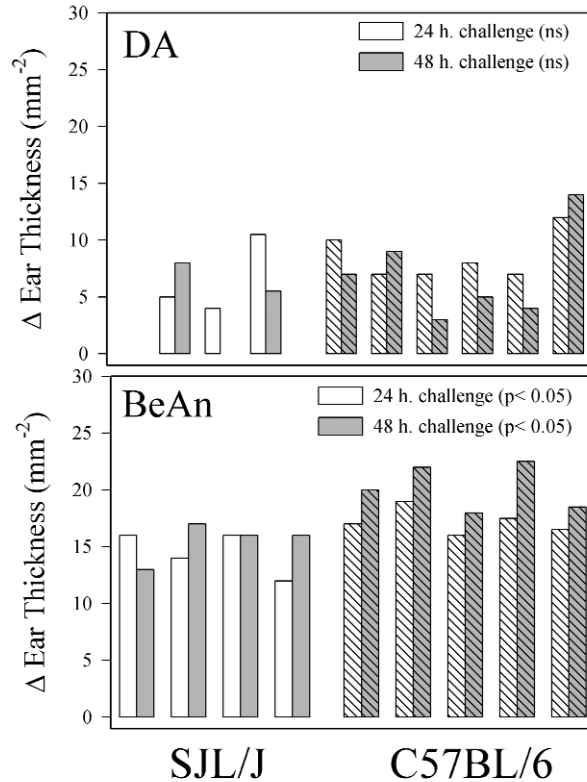

Figure 3. Delayed type hypersensitivity (DTH) responses directed against BeAn or DA antigen at 56 days following infection. Each bar represents one mouse. Data show change in ear thickness at 24- or 48-hour post antigen challenge.

virus antigen (5). We compared the DTH response in SJL/J and C57BL/6J mice infected for 56 days with either BeAn or DA (Figure 3). Because different sources and quantities of virus antigen (DA or BeAn) were used in these experiments it is not possible to directly compare the DTH response in BeAn infected versus DA infected mice. In general, greater DTH responses were observed in C57BL/6J mice as compared to SJL mice when infected with BeAn (P=0.034, 24-hour challenge and P=0.008 at the 48-hour challenge, Student's t-test). There was a trend towards a greater DTH response in DA infected C57BL/6J mice as compared to DA infected SJL/J mice (P=0.109 24-hour challenge and P=0.202 48-hour challenge), however this was not significant. Because of the lack of differences in CNS pathology and inflammation in DA and BeAn infected C57BL/6 mice further experiments focused on the pathology in DA and BeAn infected SJL mice.

Greater frequency of demyelinating disease in the spinal cords of SJL/J mice infected with DA as com-
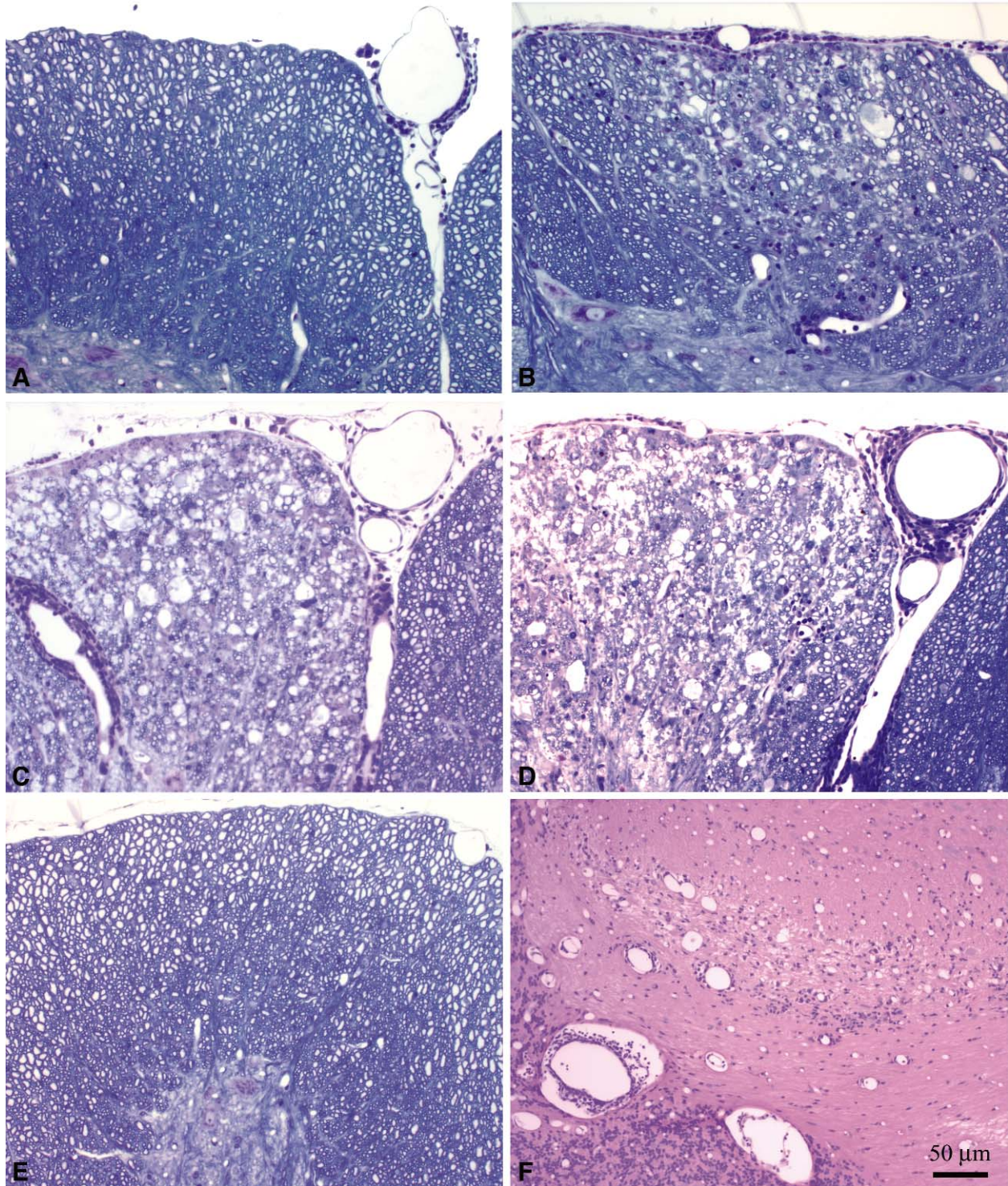
Figure 4. Spinal Cord Pathology in TMEV infected SJL/J and SJL/JCrHsd Mice **A.** SJL/J mouse infected with DA for 21 days. **B.** SJL/JCrHsd mouse infected with DA for 21 days demonstrating an increase in spinal cord demyelination. **C.** Spinal cord pathology in 45 day DA infected SJL/J mouse demonstrating extensive demyelination. **D.** BeAn infected SJL/J mouse at 45 days p.i. demonstrating similar levels of demyelination. **E.** BeAn infected SJL/J mouse at 45 days p.i. demonstrating no demyelination or inflammation in the spinal cord. **F.** Presence of brain stem and cerebellum pathology in a BeAn infected SJL/J mouse at 45 days p.i.that did not show pathology in the spinal cord.

pared to SJL/J mice infected with BeAn. We assessed the frequency of demyelination at 21, 45, 90, and 180 days post intracranial infection (Table 1). We chose these time points based on the fact that 21 days is the beginning of demyelination in the spinal cord, by 45 days demyelination is well-established, by 90 days demyelination is reaching a plateau, and by 180 days mice are showing demyelination as well as secondary axonal injury (26). At 21 days post infection, 7 of 10 DA infected SJL/J mice as compared to 2 of 10 BeAn infected SJL/J mice showed demyelination. By 45 days and 90 days, all SJL/J mice (17/17 and 10/10) infected with DA showed demyelination in the spinal cord in contrast to 21 (67.8%) of 31 and 5 (45%) of 11 SJL/J mice infected with BeAn at these time points (P<0.05 by Fisher-Exact test).

We then examined the extent of demyelination in the spinal cord of SJL/J mice following infection with these 2 strains of virus. This was done by examining 10 to 15 spinal cord blocks from each mouse and determining the number of quadrants positive for white matter inflammation and demyelination. The extent of demyelination at 21 days post infection was not statistically different between DA and BeAn infected SJL/J mice. However by 45 days there was approximately 1.3-fold increase in the number of quadrants showing demyelination in DA versus BeAn infected SJL/J mice (P=0.038 Mann-Whitney Rank Sum test). The difference was greater at 90 days when there was approximately a 4-fold increase in the number of quadrants with demyelination in DA infected SJL/J mice versus BeAn infected SJL/J mice (P= 0.006 Mann-Whitney Rank Sum test). The extent of white matter inflammation closely mirrored the extent of demyelination. No examples of gray matter inflammation or neuronal injury were observed in the spinal cord of these mice at these time points.

We then did the analysis and excluded all SJL/J mice infected with DA or BeAn, which did not show demyelination. When this was done there was no statistical difference between the extent of demyelination between DA or BeAn infected SJL/J mice at 21, 45, or 90 days following infection.

SJL/JCrHsd a show greater extent of demyelination than SJL/J mice when infected with DA. Many of the recent experiments using BeAn have used Harlan Laboratories as a source of SJL mice. We tested the possibility that one difference observed in the models was not only related to differences in the viruses but also in the hosts (Table 1, Figure 4). At 21 days there was significantly more demyelination in SJL/JCrHsd mice as com-

pared to SJL/J mice infected with DA (3.2-fold increase in demyelination, P=0.003 statistics by Student's t-test). No increase in demyelination was observed in SJL/JCrHsd mice as compared to SJL/J mice infected with BeAn at 21 days. Forty-five days after infection there was no increase in demyelination observed in SJL/JCrHsd mice as compared to SJL/J mice infected with DA (P=0.345 Student's t-test). Mice infected with BeAn virus consistently showed less demyelination as compared to mice infected with DA irrespective of the source of SJL mice. When mice which showed no demyelination were excluded from the analysis, the only significant finding was the presence of more demyelination at day 21 using DA in SJL/JCrHsd mice (14.9±2.1) as compared to SJL/J mice (6.7±2.5) (P= 0.030 Student's t-test). At the 45, 90, and 180 day time points no statistical difference was observed between demyelination in SJL/JCrHsd versus SJL/J mice infected with DA or BeAn.

Development of brain disease is similar between DA and BeAn infected mice. Having shown that there was a decreased incidence of spinal cord demyelination in BeAn infected SJL/J and SJL/JCrHsd mice, we asked whether the extent and degree of neuropathology in the brain was different between SJL/J or SJL/JCrHsd mice infected with these 2 viruses. Brain from every mouse was cut into coronal sections to allow visualization of the cerebellum, brain stem, cortex, hippocampus, striatum, corpus callosum, and meninges. The extent of neuropathology was graded on a 0 to 4 point scale as outlined in the methods. Each point in the graphs (Figure 5) represents one animal. There were no significant differences in the region of the brain showing neuropathology or in the severity of neuropathology when comparing BeAn and DA infected mice at the various time points. At 21 days following infection, severe neuropathology was frequently observed in the hippocampus and striatum. In addition, prominent meningeal infiltration was observed at 21 and 45 days following infection with either BeAn or DA. No major changes were observed when comparing SJL/J versus SJL/JCrHsd infected mice with either of these 2 viruses. Of importance, all mice infected with BeAn that showed no spinal cord demyelination still showed neuropathology in the brain (Figure 4F). Therefore, the absence of demyelination in the spinal cord was not related to early or complete clearance of virus infection from the CNS. By 45 days, clear evidence of demyelination and inflammation was observed in the cerebellum and brain stem of SJL/J and SJL/JCrHsd mice infected
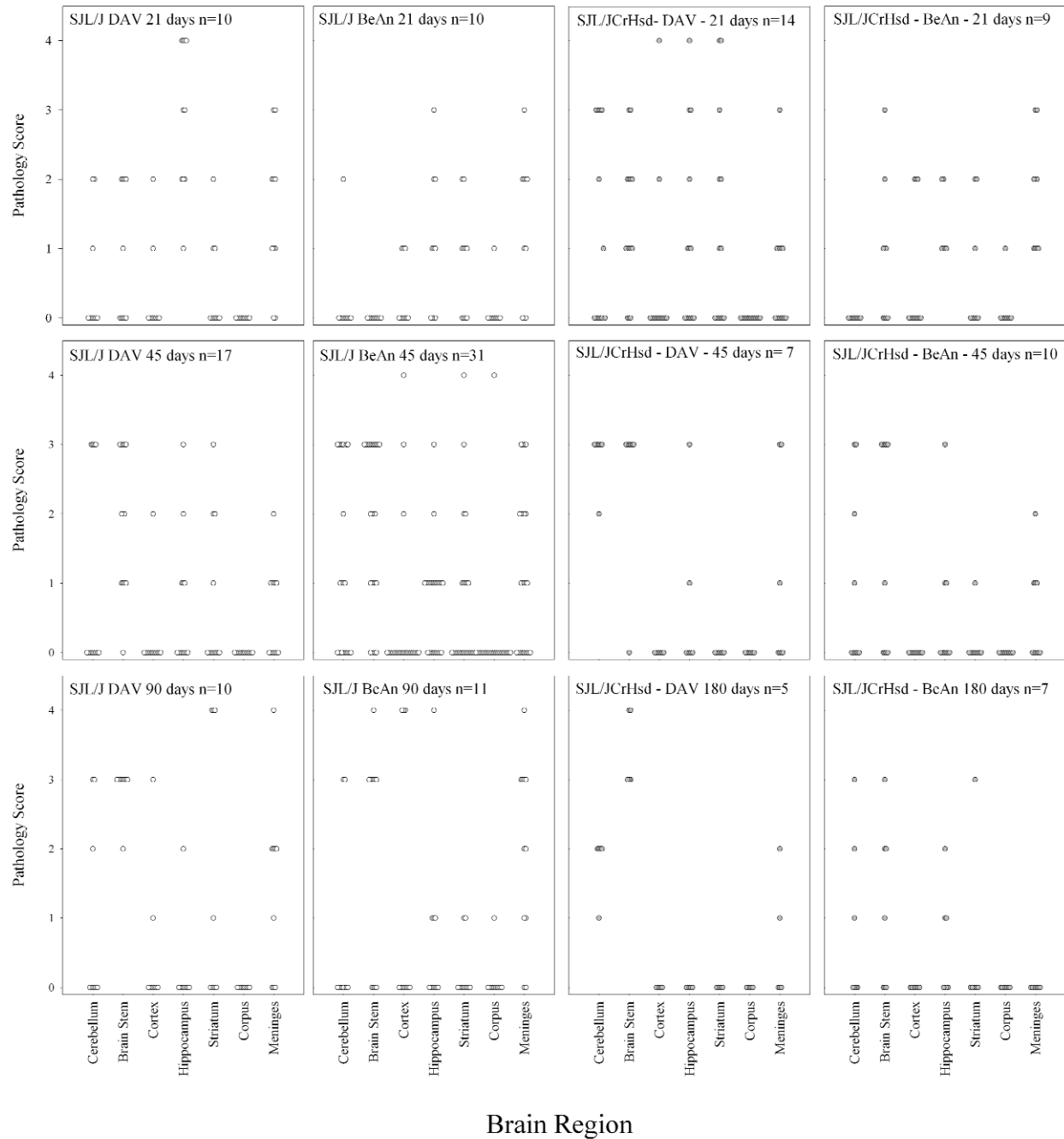
Figure 5. Pathologic scores in the brain of SJL/J or SJL/JCrHsd mice infected with DA or BeAn for 21, 45, 90, and 180 days.

with either of these 2 viruses. By 90 and 180 days following infection, most of the pathology in the hippocampus and striatum had subsided, however the pathology in brain stem progressed. Again no difference in brain neuropathology was observed in the late time points when comparing either BeAn or DA infection of either SJL/J or SJL/JCrHsd mice.

More VP2-specific viral RNA persists in the CNS of DA infected mice as compared to BeAn infected mice. Recent reports indicate that viral RNA persists follow-

Figure 6. A. Log10 virus RNA copy number (VP2) in brain or spinal cord from SJL/J mice infected with DA or BeAn for 45 days. **B.** Log10 virus RNA copy number (VP2) in the brain or spinal cord from SJL/JCrHsd mice infected with DA or BeAn for 45 days. **C.** Number of virus antigen positive cells in the spinal cord expressed per area of white matter in SJL/J mice infected with DA or BeAn for 45 or 90 days, and SJL/JCrHsd mice infected with DA or BeAn for 180 days.

ing TMEV infection during chronic disease even though it is often difficult to detect infectious virus by plaque assay (56). We developed a sensitive and quantitative RT-PCR assay that allows us to measure the copy number of VP2-specific RNA in the brain and spinal cord of DA and BeAn infected mice (Figure 6A and 6B). At 45 days following infection there was approximately 2 logs more virus-specific RNA transcripts in the spinal cord as compared to the brain of DA or BeAn infected SJL/J mice ($P < 0.05$ Student's t-test). A significant difference in copy number was observed between BeAn and DA infected SJL/J or SJL/JCrHsd mice. Approximately 2 logs more VP2 copy number was observed in DA infected mice compared to BeAn ($P < 0.05$ Student's t-test).

Virus antigen staining in the spinal cord of mice infected with DA and BeAn. We have shown previously that persistent virus antigen in the spinal cord correlates well with the degree of demyelination in the animal (48). We therefore counted the number of virus antigen positive cells per area of white matter (Figure 6C). No virus antigen positive cells were observed in the gray matter of any mouse infected with either DA or BeAn at 45, 90, and 180 days following infection. For the 45 and the 90 day time point we utilized SJL/J mice. For the 180 day time point we utilized SJL/JCrHsd mice. There was no significant difference in the number of virus antigen positive cells per area of white matter between DA (8.7 ± 1.1) and BeAn (5.4 ± 1.3) infected SJL/J mice at 45 days after infection (NS by Student's t-test). Similarly, at 90 days following infection there was a trend for greater number of virus antigen positive cells in DA infected mice (9.8 ± 1.0) as compared to BeAn infected mice (3.9 ± 2.0) (NS by Student's t-test). However 180 days after infection of SJL/JCrHsd mice, there was 4 times more antigen positive cells observed in mice infected with DA (16.0 ± 3.4) as compared to BeAn (3.9 ± 2.0) which was statistically significant ($P = 0.02$ by Student's t-test).

Virus antigen localization in the spinal cord and brain stem of DA and BeAn infected mice. We identi-
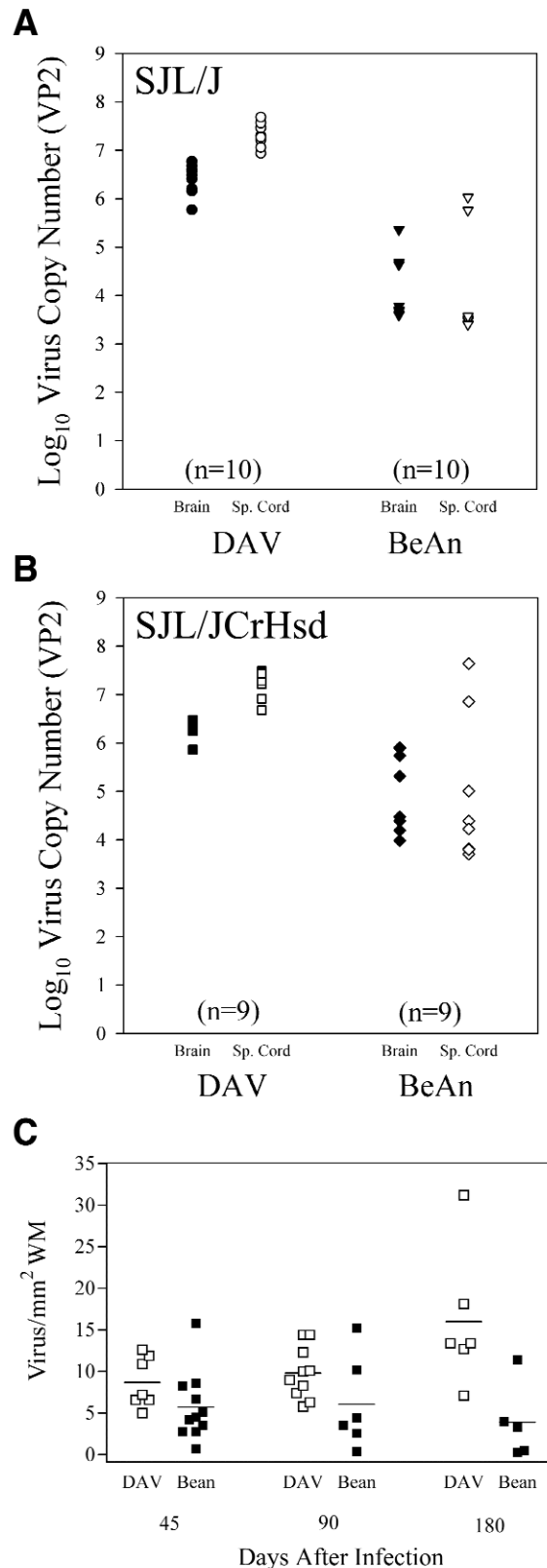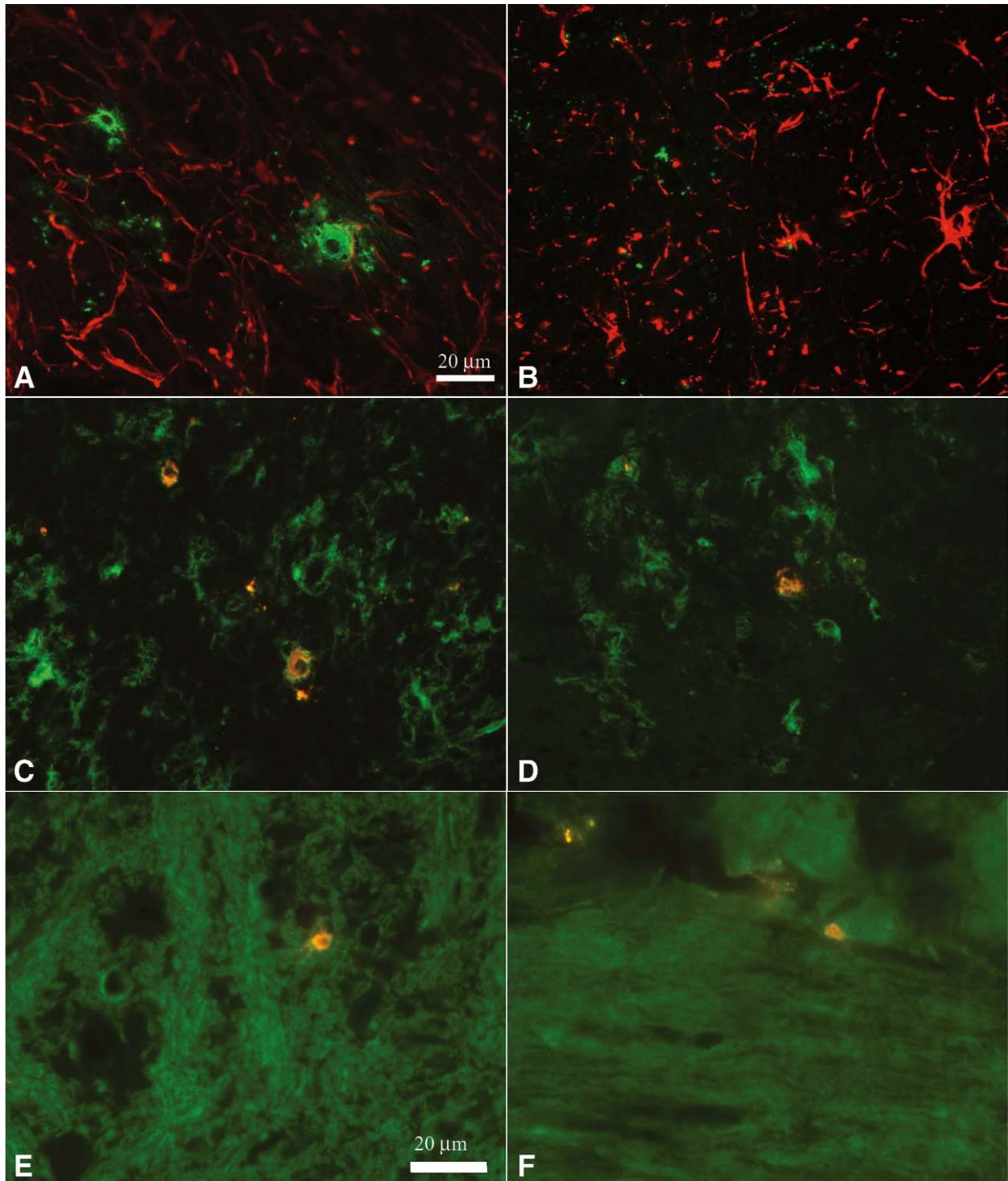
Figure 7. Double-labeling immunoflourescence of virus infected cells in the CNS of mice infected with TMEV for 45 or 90 days. GFAP positive cells (red) do not localize to virus antigen (green) in 45 day infected (**A**) DA or (**B**) BeAn spinal cord sections (40X). F4/80 labeled cells (green) demonstrate colocalization with virus (yellow) in 45 day infected (**C**) DA and (**D**) BeAn brainstem sections (40×). Oligodendrocytes positive for CNPase (green) are positive for TMEV antigen (yellow) in both 45 day infected E)DA and 90 day infected F) BeAn brainstem sections (60×).

fied the cells expressing virus antigen in the spinal cord and brain stem of mice infected with DA or BeAn using a double labeling immunoflourescence technique (Figure 7). For these experiments, frozen sections were cut from SJL/J mice infected for 45 and 90 days with either DA or BeAn and used for staining. We used an antibody to glial-fibrillary acidic protein (GFAP) to identify astrocytes, the antibody F4/80 to identify microglia/macrophages and an antibody to CNPase to identify oligodendrocytes. No virus infected astrocytes were observed following infection with either BeAn or DA. In contrast a number of F4/80+ macrophage/ microglial cells contained virus antigen following infection with either BeAn or DA, demonstrating that these cells were actively infected or had phagocytosed viral antigen debris. In addition, we saw cells positive for CNPase that colocalized with virus antigen after infection with either DA or BeAn.

TMEV specific IgG ELISA for DA and BeAn infected SJL mice. DA and BeAn specific IgG ELISA for DA and BeAn infected SJL/J mice were performed on mice that were chronically infected with TMEV for 58 and 90 days (Figure 8). Both the DA and the BeAn specific ELISA demonstrated a difference in IgG's when comparing the two different viral infections. The BeAn infected animals showed an increased titer to both DA and BeAn (P<0.05 Repeated Measures ANOVA with pairwise comparison by Student-Newman-Keuls).

Functional deficits following DA versus BeAn infection of SJL/JCrHsd mice. We have shown previously that it is possible to objectively measure neurological deficits in DA infected SJL/J mice using rotarod assay, footprint analysis, or spontaneous activity monitors (14, 27, 44). We performed a time course experiment following DA and BeAn infected SJL/JCrHsd mice. We chose to study functional deficits in SJL/JCrHsd mice because of the higher incidence and severity of spinal cord demyelination observed in these mice following early infection. For these experiments SJL/JCrHsd mice infected for 24 to 29 days were compared to mice infected for 46, 99, and 191 days (Figure 9). Both DA and BeAn infected mice showed progressive motor deficits as a function of time (P<0.05 by One Way ANOVA). However, as the disease progressed, more severe functional deficits were observed in DA infected SJL/JCrHsd mice as compared to the BeAn infected SJL/JCrHsd mice (P<0.05 by Two Way ANOVA, pairwise comparisons using Tukey's test). We compared the
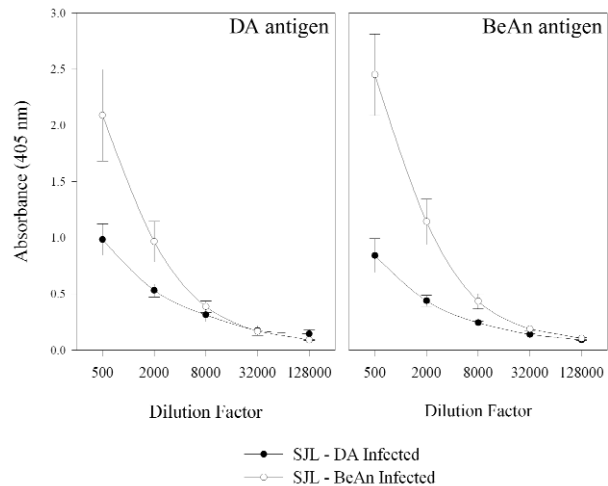

Figure 8. DA and BeAn specific IgG ELISA of sera from chronically infected SJL/J mice. **A.** BeAn infected SJL/J mice show an increased IgG titer to DA antigen when compared to DA infected SJL/J mice (P<0.05 Mann-Whitney Rank Sum test). **B.** BeAn infected SJL/J mice demonstrate increased IgG titer to BeAn antigen when compared to DA infected SJL/J mice.
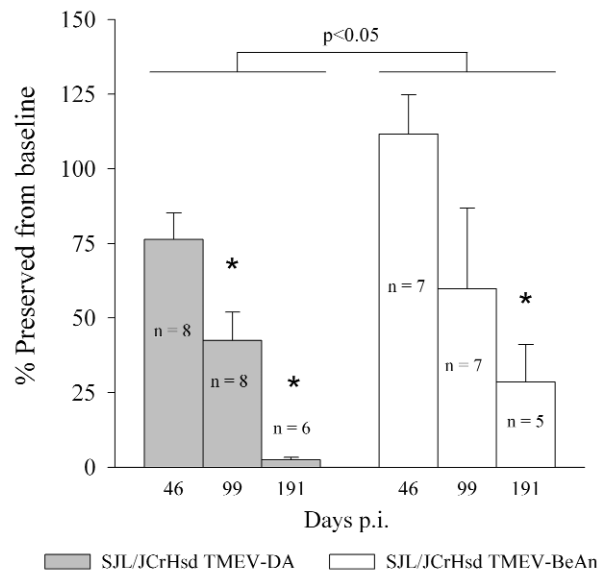

Figure 9. Functional deficits as measured by ROTAROD assay of SJL/JCrHsd mice infected with DA versus BeAn for 46, 99, and 191 days. Asterisk shows statistically significant decrease in function P<0.05.

function of these mice to the 24-day data to evaluate the functional deficits secondary to the demyelinating disease and therefore exclude any functional deficits from the early encephalitic phase of the disease. However, there was no difference in the function of DA infected versus BeAn infected SJL/JCrHsd mice at 24 days following

Virus	98	99	100	101	Amino Acid Position 102	102a	102b	103	104	105	Demyelination	Reference
GDVII	S	G	G	A	N	G	A	N	F	P	-	(15, 41)
DA	S	G	G	T	T	-	-	N	F	P	+	(36)
BeAn	S	G	G	V	N	G	A	N	F	P	+	(42)
WW	S	G	G	T	T	-	-	N	F	P	+	(30)
Yale	S	G	G	A	N	G	A	N	F	P	+	(30)
DA9	S	G	G	T	T	G	A	N	F	P	-	(58)
DA8	S	G	G	A	N	G	A	N	F	P	+	(58)
Osm101	S	G	G	I	T	-	-	N	F	P	-	(60)
DA3304	S	G	G	A	T	-	-	N	F	P	+	(59)
DA-VP1-99(Ser)	S	S	G	T	T	-	-	N	F	P	-	(17, 49)
DA-VP1-100(Asp)	S	G	D	T	T	-	-	N	F	P	-	(17, 49)
DA-VP1-103(Lys)	S	G	G	T	T	-	-	K	F	P	+	(17, 49)

Table 2. VP1 Loop II mutants of DA or BeAn cited in the literature.

infection. The average speed (RPM) of rotarod at the time of fall was 21.7 ± 1.6 in DA infected mice and 20.8 ± 2.6 in BeAn infected mice (NS by Student's t-test). As shown previously neurological deficits continued to worsen after 99 days of infection in spite of the fact that the incidence of demyelination in the spinal cord and extent of demyelination was similar between the 90 and 180 day time point. This is consistent with the hypothesis that secondary injury to axons may contribute to neurological deficits in both DA and BeAn infected SJL/JCrHsd mice, as has been shown previously in DA infected SJL/J mice(26).

Discussion

This is the first manuscript to report a direct comparison of the CNS pathology of the 2 most commonly used models of TMEV-induced demyelination. Investigators have used both the Daniel's strain and the BeAn 8386 strain in SJL mice. Furthermore, SJL mice have been obtained from different sources. In this study, our goal was to compare the models as have been used previously by the investigators in the field. Therefore we chose to infect with 2×10^6 pfu of DA and 1.5×10^6 pfu of BeAn. We suspect that this minor difference in input virus is likely within the standard error of plaque assay and does not account for the difference in the incidence of demyelination in the spinal cord observed with these viruses. However, qualitatively the plaque assays demonstrated that DA was clearly more lytic to L2 cells than BeAn by producing larger plaques. This would suggest that there might be an important difference in the replication of these viruses and their ability to lyse cells.

The data support the conclusion that DA is more virulent than BeAn virus. This is supported by a higher fre-

quency and extent of demyelination in the spinal cord, more virus antigen positive cells during chronic stages of disease, and higher level of virus-specific RNA (VP2) in the CNS in DA versus BeAn infected mice. Thus DA has a greater propensity to infect the spinal cord white matter and result in subsequent inflammatory demyelination. However, virulence likely is not the only explanation since the extent of brain pathology and distribution of brain lesions were similar between DA and BeAn infected mice. Of particular interest were mice that showed no demyelination in the spinal cord even after analysis of 15 to 20 sequential sections encompassing the entire cord. All of these mice showed brain pathology. This would argue that the mechanism for induction of brain pathology versus spinal cord demyelination may be distinct in BeAn infected mice. This contrasts with DA infected mice where there was a stronger relationship between brain and spinal cord pathology.

One unexpected but very interesting finding was the observation of greater demyelination in SJL/JCrHsd mice as compared to SJL/J mice. SJL/JCrHsd mice showed much earlier demyelination in the spinal cord only after infection with DA. It has been previously assumed that these mouse strains are genetically identical. However, the increased incidence and severity of early demyelination in SJL/JCrHsd mice following DA infection and the reported greater development of autoimmunity to myelin antigens in these mice (37) suggest that there are important genetic differences as relates to demyelination in these mice. This parallels previously published data by Nicholson et al (32) that shows differences between BALB/c substrains in their susceptibility to TMEV induced demyelination. Further evidence in the 129 strain (53) has demonstrated that genetic variability should be considered when compar-

ing substrains of mice. Since these SJL strains are very closely related and their genes highly conserved, this may provide a unique opportunity to determine those genes important in controlling earlier and increased incidence of demyelination following TMEV infection.

Unknown are the genes of TMEV that determine the difference in the pathologic and clinical phenotype following infection with DA versus BeAn. Much is known regarding the differences between the highly neurovirulent (GDVII) strain and either DA or BeAn. Multiple recombinant viruses encompassing GDVII and DA (12, 25, 46) and GDVII and BeAn (1, 59) have been described. The data suggest that neurovirulence from GDVII virus infection maps primarily to the viral capsid antigens and in particular VP1. It is possible that similar differences in demyelination between DA and BeAn may also map to the viral capsid antigens. Previous work has shown that the areas of least homology appear to reside in the leader (L) peptide and VP1 of DA and BeAn (36). Future recombinant viruses between DA and BeAn could help answer this important question.

One possibility for the attenuated phenotype seen in the BeAn strain of virus compared to DA could be the differences in amino acid composition around the VP1 loop II region. This region comprises amino acids 98 through 105 of the VP1 capsid and is thought to be a critical receptor binding region. Several mutant TMEV viruses have been generated with changes in this region that have affected the incidence of demyelination (Table 2). Of interest is the vulnerability of amino acid 101 to change and the induction of attenuated phenotypes seen in vivo as well as in vitro. For example, a change from threonine to alanine or isoleucine at position 101 in VP1 results in attenuated phenotypes in infected SJL mice (58). Furthermore when 2 amino acids were inserted (G and A) after the threonine at position 102, thus making the DA more "BeAn-like," this also generated a disease phenotype that failed to induce clinical symptoms when compared to wild type DA (57). Evidence from other studies shows that changes at residues 99, 100 and 103 can change the course of infection in SJL mice (17). Although these are not direct changes to the 101 site, changes at these sites may generate viruses that are morphologically different due to side chain interactions of the amino acids and overall changes in folding at this potential receptor binding site. In vitro evidence in L2 cells also supports the attenuation of phenotype in VP1 loop II mutants. Infection of L2 cells with mutations at VP1-99, VP1-100 and VP1-103 resulted in a reduction of plaque sizes in L2 monolayers (17). This decrease in plaque size was similar to those observed in the present study when comparing DA and BeAn. The data support the hypothesis that the differences observed in the VP1 loop II region between DA and BeAn could be contributing to a reduced ability to interact with the cellular receptor in spinal cord white matter and generate a less productive infection with decreased incidence of demyelination and neurologic deficits.

Of particular interest were the functional assays using the rotarod to determine chronic neurologic deficits in TMEV infected mice. In this study we investigated SJL/JCrHsd mice infected with DA or BeAn because of the earlier development of demyelination especially after DA infection. The data showed that particularly during the later stages of disease (90-180 days), DA infected SJL/JCrHsd mice showed more severe functional deficits as compared to BeAn infected SJL/JCrHsd mice. We have performed similar experiments previously using DA infection in SJL/J mice (26). When comparing the previous published results with those of the present study it is clear that both BeAn infected and DA infected SJL/JCrHsd mice have more functional deficits than DA infected SJL/J mice.

The data suggest that DA and BeAn induced CNS diseases are distinct. DA being the more lytic virus appears to result in greater frequency of spinal cord demyelination and greater extent of demyelination especially as the disease progresses. This may be due to direct viral injury of glial cells or an immune response against these cells. In contrast, BeAn appears to be less virulent. This may predispose this virus toward development of CD4+ T-cell mediated delayed-type hypersensitivity responses directed against virus antigen which later spreads to myelin antigen to contribute to demyelination (31). In addition, there may be unique genetic contributions of the SJL/JCrHsd strain that predisposes this mouse strain to autoimmunity. Finally, the detailed analysis of brain pathology induced following infection with these viruses raises the hypothesis that demyelination in the spinal cord as well as lesions in the brain stem may contribute to the neurological deficits observed in these mice.

References

1. Adami C, Pritchard AE, Knauf T, Luo M, Lipton HL (1998) A determinant for central nervous system persistence localized in the capsid of Theiler's murine encephalomyelitis virus by using recombinant viruses. *J Virol* 72:1662-1665.

2. Azoulay-Cayla A, Dethlefs S, Perarnau B, Larsson-Sciard EL, Lemonnier FA, Brahic M, Bureau JF (2000) H-2D(b-/-) mice are susceptible to persistent infection by Theiler's virus. *J Virol* 74:5470-5476.

3. Azoulay A, Brahic M, Bureau JF (1994) FVB mice transgenic for the H-2Db gene become resistant to persistent infection by Theiler's virus. *J Virol* 68:4049-4052.

4. Borson ND, Paul C, Lin X, Nevala WK, Strausbauch MA, Rodriguez M, Wettstein PJ (1997) Brain-infiltrating cytolytic T lymphocytes specific for Theiler's virus recognize H2Db molecules complexed with a viral VP2 peptide lacking a consensus anchor residue. *J Virol* 71:5244-5250.

5. Clatch RJ, Lipton HL, Miller SD (1986) Characterization of Theiler's murine encephalomyelitis virus (TMEV)-specific delayed-type hypersensitivity responses in TMEV-induced demyelinating disease: correlation with clinical signs. *J Immunol* 136:920-927.

6. Clatch RJ, Lipton HL, Miller SD (1987) Class II-restricted T-cell responses in Theiler's murine encephalomyelitis virus (TMEV)-induced demyelinating disease. II. Survey of host immune responses and central nervous system virus titers in inbred mouse strains. *Microb Pathog* 3:327-337.

7. Clatch RJ, Melvold RW, Miller SD, Lipton HL (1985) Theiler's murine encephalomyelitis virus (TMEV)-induced demyelinating disease in mice is influenced by the H-2D region: correlation with TEMV-specific delayed-type hypersensitivity. *J Immunol* 135:1408-1414.

8. Dal Canto MC, Melvold RW, Kim BS, Miller SD (1995) Two models of multiple sclerosis: experimental allergic encephalomyelitis (EAE) and Theiler's murine encephalomyelitis virus (TMEV) infection. A pathological and immunological comparison. *Microsc Res Tech* 32:215-29.

9. Dethlefs S, Escriou N, Brahic M, van der WS, Larsson-Sciard EL (1997) Theiler's virus and Mengo virus induce cross-reactive cytotoxic T lymphocytes restricted to the same immunodominant VP2 epitope in C57BL/6 mice. *J Virol* 71:5361-5365.

10. Drescher KM, Murray PD, David CS, Pease LR, Rodriguez M (1999) CNS cell populations are protected from virus-induced pathology by distinct arms of the immune system. *Brain Pathol* 9:21-31.

11. Friedmann A, Frankel G, Lorch Y, Steinman L (1987) Monoclonal anti-I-A antibody reverses chronic paralysis and demyelination in Theiler's virus-infected mice: critical importance of timing of treatment. *J Virol* 61:898-903.

12. Jnaoui K, Minet M, Michiels T (2002) Mutations that affect the tropism of DA and GDVII strains of Theiler's virus in vitro influence sialic acid binding and pathogenicity. *J Virol* 76:8138-8147.

13. Johnson AJ, Njenga MK, Hansen MJ, Kuhns ST, Chen L, Rodriguez M, Pease LR (1999) Prevalent class I-restricted T-cell response to the Theiler's virus epitope Db:VP2121-130 in the absence of endogenous CD4 help, tumor necrosis factor alpha, gamma interferon, perforin, or costimulation through CD28. *J Virol* 73:3702-3708.

14. Johnson AJ, Upshaw J, Pavelko KD, Rodriguez M, Pease LR (2001) Preservation of motor function by inhibition of CD8+ virus peptide-specific T-cells in Theiler's virus infection. *FASEB J* 15:2760-2762.

15. Law KM, Brown TD (1990) The complete nucleotide sequence of the GDVII strain of Theiler's murine encephalomyelitis virus (TMEV). *Nucleic Acids Res* 18:6707-6708.

16. Lehrich JR, Arnason BG, Hochberg FH (1976) Demyelinative myelopathy in mice induced by the DA virus. *J Neurol Sci* 29:149-160.

17. Lin X, Sato S, Patick AK, Pease LR, Roos RP, Rodriguez M (1998) Molecular characterization of a nondemyelinating variant of Daniel's strain of Theiler's virus isolated from a persistently infected glioma cell line. *J Virol* 72:1262-1269.

18. Lindsley MD, Rodriguez M (1989) Characterization of the inflammatory response in the central nervous system of mice susceptible or resistant to demyelination by Theiler's virus. *J Immunol* 142:2677-2682.

19. Lindsley MD, Thiemann R, Rodriguez M (1991) Cytotoxic T-cells isolated from the central nervous systems of mice infected with Theiler's virus. *J Virol* 65:6612-6620.

20. Lipton HL (1980) Persistent Theiler's murine encephalomyelitis virus infection in mice depends on plaque size. *J Gen Virol* 46:169-177.

21. Lipton HL, Dal Canto MC (1976) Chronic neurologic disease in Theiler's virus infection of SJL/J mice. *J Neurol Sci* 30:201-207.

22. Lipton HL, Melvold R (1984) Genetic analysis of susceptibility to Theiler's virus-induced demyelinating disease in mice. *J Immunol* 132:1821-1825.

23. Lipton HL, Twaddle G, Jelachich ML (1995) The predominant virus antigen burden is present in macrophages in Theiler's murine encephalomyelitis virus-induced demyelinating disease. *J Virol* 69:2525-2533.

24. Lorch Y, Friedmann A, Lipton HL, Kotler M (1981) Theiler's murine encephalomyelitis virus group includes two distinct genetic subgroups that differ pathologically and biologically. *J Virol* 40:560-567.

25. McAllister A, Tangy F, Aubert C, Brahic M.J (1990) Genetic mapping of the ability of Theiler's virus to persist and demyelinate. *Virology* 64(9):4252-7.

26. McGavern DB, Murray PD, Rivera-Quinones C, Schmelzer JD, Low PA, Rodriguez M (2000) Axonal loss results in spinal cord atrophy, electrophysiological abnormalities and neurological deficits following demyelination in a chronic inflammatory model of multiple sclerosis. *Brain* 123 Pt 3:519-531.

27. McGavern DB, Zoecklein L, Drescher KM, Rodriguez M (1999) Quantitative assessment of neurologic deficits in a chronic progressive murine model of CNS demyelination. *Exp Neurol* 158:171-181.

28. Melero I, Singhal MC, McGowan P, Haugen HS, Blake J, Hellstrom KE, Yang G, Clegg CH, Chen L (1997) Immunological ignorance of an E7-encoded cytolytic T-lymphocyte epitope in transgenic mice expressing the E7 and E6 oncogenes of human papillomavirus type 16. *J Virol* 71:3998-4004.

29. Melvold RW, Jokinen DM, Knobler RL, Lipton HL (1987) Variations in genetic control of susceptibility to Theiler's murine encephalomyelitis virus (TMEV)-induced demyelinating disease. I. Differences between susceptible SJL/J and resistant BALB/c strains map near the T-cell beta-chain constant gene on chromosome 6. *J Immunol* 138:1429-1433.

30. Michiels T, Jarousse N, Brahic M (1995) Analysis of the leader and capsid coding regions of persistent and neurovirulent strains of Theiler's virus. *Virology* 214:550-558.

31. Neville KL, Padilla J, Miller SD (2002) Myelin-specific tolerance attenuates the progression of a virus-induced demyelinating disease: implications for the treatment of MS. *J Neuroimmunol* 123:18-29.

32. Nicholson SM, Peterson JD, Miller SD, Wang K, Dal Canto MC, Melvold RW (1994) BALB/c substrain differences in susceptibility to Theiler's murine encephalomyelitis virus-induced demyelinating disease. *J Neuroimmunol* 52:19-24.

33. Njenga MK, Asakura K, Hunter SF, Wettstein P, Pease LR, Rodriguez M (1997) The immune system preferentially clears Theiler's virus from the gray matter of the central nervous system. *J Virol* 71:8592-8601.

34. Njenga MK, Pavelko KD, Baisch J, Lin X, David C, Leibowitz J, Rodriguez M (1996) Theiler's virus persistence and demyelination in major histocompatibility complex class II-deficient mice. *J Virol* 70:1729-1737.

35. Noseworthy JH, Lucchinetti C, Rodriguez M, Weinshenker BG (2000) Multiple sclerosis. *N Engl J Med* 343(13):938-52.

36. Ohara Y, Stein S, Fu JL, Stillman L, Klaman L, Roos RP (1988) Molecular cloning and sequence determination of DA strain of Theiler's murine encephalomyelitis viruses. *Virology* 164:245-255.

37. Olson JK, Croxford JL, Calenoff MA, Dal Canto MC, Miller SD (2001) A virus-induced molecular mimicry model of multiple sclerosis. *J Clin Invest* 108:311-318.

38. Patick AK, Oleszak EL, Leibowitz JL, Rodriguez M (1990) Persistent infection of a glioma cell line generates a Theiler's virus variant which fails to induce demyelinating disease in SJL/J mice. *J Gen Virol* 71:2123-2132.

39. Pavelko KD, Drescher KM, McGavern DB, David CS, Rodriguez M (2000) HLA-DQ polymorphism influences progression of demyelination and neurologic deficits in a viral model of multiple sclerosis. *Mol Cell Neurosci* 15:495-509.

40. Paya CV, Patick AK, Leibson PJ, Rodriguez M (1989) Role of natural killer cells as immune effectors in encephalitis and demyelination induced by Theiler's virus. *J Immunol* 143:95-102.

41. Pevear DC, Borkowski J, Calenoff M, Oh CK, Ostrowski B, Lipton HL (1988) Insights into Theiler's virus neurovirulence based on a genomic comparison of the neurovirulent GDVII and less virulent BeAn strains. *Virology* 165:1-12.

42. Pevear DC, Calenoff M, Rozhon E, Lipton HL (1987) Analysis of the complete nucleotide sequence of the picornavirus Theiler's murine encephalomyelitis virus indicates that it is closely related to cardioviruses. *J Virol* 61:1507-1516.

43. Pierce ML, Rodriguez M (1989) Erichrome stain for myelin on osmicated tissue embedded in glycol methacrylate plastic. *J Histotechnol* 12:35-36.

44. Rivera-Quinones C, McGavern D, Schmelzer JD, Hunter SF, Low PA, Rodriguez M (1998) Absence of neurological deficits following extensive demyelination in a class I-deficient murine model of multiple sclerosis. *Nat Med* 4:187-193.

45. Rodriguez M, David CS (1995) H-2 Dd transgene suppresses Theiler's virus-induced demyelination in susceptible strains of mice. *J Neurovirol* 1:111-117.

46. Rodriguez M, Leibowitz J, David CS (1986) Susceptibility to Theiler's virus-induced demyelination. Mapping of the gene within the H-2D region. *J Exp Med* 163:620-631.

47. Rodriguez M, Leibowitz JL, Lampert PW (1983) Persistent infection of oligodendrocytes in Theiler's virus-induced encephalomyelitis. *Ann Neurol* 13:426-433.

48. Rodriguez M, Pavelko KD, Njenga MK, Logan WC, Wettstein PJ (1996) The balance between persistent virus infection and immune cells determines demyelination. *J Immunol* 157:5699-5709.

49. Rodriguez M, Roos RP, McGavern D, Zoecklein L, Pavelko K, Sang H, Lin X (2000) The CD4-mediated immune response is critical in determining the outcome of infection using Theiler's viruses with VP1 capsid protein point mutations. *Virology* 275:9-19.

50. Rossi CP, Delcroix M, Huitinga I, McAllister A, van Rooijen N, Claassen E, Brahic M.J (1997) Role of macrophages during Theiler's virus infection. *Virology* 71(4):3336-40.

51. Sethi P, Lipton HL (1983) Location and distribution of virus antigen in the central nervous system of mice persistently infected with Theiler's virus. *Br J Exp Pathol* 64:57-65.

52. Simas JP, Fazakerley JK (1996) The course of disease and persistence of virus in the central nervous system varies between individual CBA mice infected with the BeAn strain of Theiler's murine encephalomyelitis virus. *J Gen Virol* 77 (Pt 11):2701-2711.

53. Simpson EM, Linder CC, Sargent EE, Davisson MT, Mobraaten LE, Sharp JJ (1997) Genetic variation among 129 substrains and its importance for targeted mutagenesis in mice. *Nat Genet* 16:19-27.

54. Tompkins SM, Fuller KG, Miller SD (2002) Theiler's virus-mediated autoimmunity: local presentation of CNS antigens and epitope spreading. *Ann N Y Acad Sci* 958:26-38.

55. Trottier M, Kallio P, Wang W, Lipton HL (2001) High numbers of viral RNA copies in the central nervous system of mice during persistent infection with Theiler's virus. *J Virol* 75:7420-7428.

56. Trottier M, Schlitt BP, Lipton HL (2002) Enhanced detection of Theiler's virus RNA copy equivalents in the mouse central nervous system by real-time RT-PCR. *J Virol Methods* 103:89-99.

57. Wada Y, McCright IJ, Whitby FG, Tsunoda I, Fujinami RS (1998) Replacement of loop II of VP1 of the DA strain with loop II of the GDVII strain of Theiler's murine encephalomyelitis virus alters neurovirulence, viral persistence, and demyelination. *J Virol* 72:7557-7562.

58. Wada Y, Pierce ML, Fujinami RS (1994) Importance of amino acid 101 within capsid protein VP1 for modulation of Theiler's virus-induced disease. *J Virol* 68:1219-1223.

59. Zhou L, Lin X, Green TJ, Lipton HL, Luo M (1997) Role of sialyloligosaccharide binding in Theiler's virus persistence. *J Virol* 71:9701-9712.

60. Zurbriggen A, Thomas C, Yamada M, Roos RP, Fujinami RS (1991) Direct evidence of a role for amino acid 101 of VP-1 in central nervous system disease in Theiler's murine encephalomyelitis virus infection. *J Virol* 65:1929-1937.